STATE TRANSITIONS IN THE GREEN ALGA *SCENEDESMUS OBLIQUUS* PROBED BY TIME-RESOLVED CHLOROPHYLL FLUORESCENCE SPECTROSCOPY AND GLOBAL DATA ANALYSIS

JOACHIM WENDLER AND ALFRED R. HOLZWARTH
Max-Planck-Institut für Strahlenchemie, D-4330 Mülheim/Ruhr, West Germany

ABSTRACT Decay-associated fluorescence spectra of the green alga *Scenedesmus obliquus* have been measured by single-photon timing with picosecond resolution in various states of light adaptation. The data have been analyzed by applying a global data analysis procedure. The amplitudes of the decay-associated spectra allow a determination of the relative antenna sizes of the photosystems. We arrive at the following conclusions: (*a*) The fluorescence kinetics of algal cells with open PS II centers (F_0 level) have to be described by a sum of three exponential components. These decay components are attributed to photosystem (PS) I ($\tau \approx 85$ ps, $\lambda_{max}^{em} \approx 695$–700 nm), open PS II α-centers ($\tau \approx 300$ ps, $\lambda_{max}^{em} = 685$ nm), and open PS II β-centers ($\tau \approx 600$ ps, $\lambda_{max}^{em} = 685$ nm). A fourth component of very low amplitude ($\tau \approx 2.2$–2.3 ns, $\lambda_{max}^{em} = 685$ nm) derives from dead chlorophyll. (*b*) At the F_{max} level of fluorescence there are also three decay components. They originate from PS I with properties identical to those at the F_0 level, from closed PS II α-centers ($\tau \approx 2.2$ ns, $\lambda_{max}^{em} = 685$ nm) and from closed PS β-centers ($\tau \approx 1.2$ ns, $\lambda_{max}^{em} = 685$ nm). (*c*) The major effect of light-induced state transitions on the fluorescence kinetics involves a change in the relative antenna size of α- and β-units brought about by the reversible migration of light-harvesting complexes between α-centers and β-centers. (*d*) A transition to state II does not measurably increase the direct absorption cross-section (antenna size) of PS I. Our data can be rationalized in terms of a model of the antenna organization that relates the effects of state transitions and light-harvesting complex phosphorylation with the concepts of PS II α,β-heterogeneity. We discuss why our results are in disagreement with those of a recent lifetime study of *Chlorella* by M. Hodges and I. Moya (1986, *Biochim. Biophys. Acta.*, 849:193–202).

INTRODUCTION

Time-resolved fluorescence spectroscopy on the picosecond time scale on photosynthetic membranes can provide detailed information on such parameters as energy transfer kinetics and pathways, the spectra of the connected antenna, relative absorption cross-sections of the different photosystems, variations in communication between photosynthetic units, spill-over, and redox state of the reaction centers (for recent reviews see references 1 and 2). This technique thus could provide a powerful tool for the study of the functional organization of photosynthetic membranes, e.g., photosystem (PS) II heterogeneity (3, 4), or the processes related to state transitions and thylakoid phosphorylation (5, 6). Previous picosecond studies resolved the fluorescence decay into three exponentials (7–13). Analysis in terms of three or more decay components is highly demanding both on the quality of the data themselves and the data analysis procedures. To solve this basic problem of the analysis of fluorescence decay curves we improved data analysis by making use of a newly developed global data analysis technique that greatly enhances the capability for multicomponent resolution and enables a much clearer differentiation between different kinetic models (14, 15).

State transitions in oxygenic photosynthesis provide a regulatory mechanism to maintain optimum quantum efficiency of noncyclic electron transport in response to changes in external light conditions. They have first been reported by Bonaventura and Myers (16) and Murata (17) (for a recent review see reference 18). State transitions have recently been studied in green algae (19–23) and in leaves and chloroplasts of higher plants (24–27). The characteristics of these transitions are changes in oxygen evolution efficiency (16, 28, 29), in chlorophyll (Chl) fluorescence induction curves (20–22, 30, 31), and in the far-red/red ratio in low temperature Chl fluorescence (17, 19, 21, 32). The current explanation of these processes in higher plants and green algae involves a redistribution of light energy between PS II and PS I brought about by reversible phosphorylation of the light-harvesting complex (LHCP) (18, 22, 32–35). Upon overexcitation of PS II, a

All correspondence should be addressed to Dr. Holzwarth.

situation, termed state II, develops that is characterized by a phosphorylated LHCP, a decreased PS II activity, a lowered variable fluorescence (F_{var}), and an increased energy transfer to PS I (for reviews see references 36–38).

The latter could be caused by one or both of the following phenomena: Increase in spill-over (energy transfer) from PS II–attached pigments to PS I (39, 40) and/or a direct increase in PS I absorption cross-section due to attachment of the phosphorylated LHCP to the PS I antenna (35, 36, 40–42). In view of the long-standing controversies in the literature on the mechanism underlying state transitions there is a need for experiments suitable to separate the effects of changes in direct PS I absorption cross-section on the one hand and spill-over effects on the other hand.

There exists much experimental data indicating that PS II is heterogeneous, consisting of two types of reaction center/antenna complexes called α-units and β-units (43–47). Evidence for this type of heterogeneity comes mainly from the biphasic Q reduction kinetics (44, 48–51) and from PS II Chl fluorescence induction (43, 52). According to current understanding PS II α-units should be located in the stacked regions of the thylakoids, forming a matrix system that involves a large part of LHCP. The PS II β-units are believed to be located in the stroma-exposed regions of the thylakoids (53, 54), to carry a smaller equivalent of LHCP, and behave as isolated units. Some of the interpretations referring to α- and β-heterogeneity have been criticized also recently (55). In particular a recent time-resolved fluorescence study questioned the assignment of the two PS II lifetime components to α- and β-units (56). For this reason further studies on this subject were also desirable.

The purpose of the present paper is severalfold: (*a*) to demonstrate the influence of state transitions in green algae on the fluorescence decay parameters and decay-associated fluorescence spectra, (*b*) to further investigate the PS I contribution to the fluorescence kinetics (3, 4), and (*c*) to gain closer insight into the suggested PS II α,β-heterogeneity. By choosing favorable experimental conditions, particular emphasis has been given to a strict control of the light state of the cells during the measurements. We have carried out these studies on the green alga *Scenedesmus obliquus* in view of the large body of data on photosynthetic parameters that is available for this alga in the literature. These studies also involve synchronous cultures of *Scenedesmus*, which we have begun to study by time-resolved spectroscopy.

MATERIALS AND METHODS

Wild-type *Scenedesmus obliquus* have been grown under continuous white light illumination in Kesslers medium modified according to Bishop and Senger (57) supplied with ≈3% CO_2-enriched air. The cells were harvested during the logarithmic growth phase and used for fluorescence measurements after dilution to ≈15 μg/ml Chl with growth medium. For chlorophyll determination the cells were extracted in hot methanol. The Chl concentration was calculated using the equations of Holden (58) and the absorption coefficients of MacKinney (59).

Picosecond fluorescence measurements were performed using a synchronously pumped, cavity-dumped dye laser system with a mode-locked argon ion laser (Spectra-Physics Inc., Mountain View, CA) as the pumping source. This system emits light pulses of typically 10-ps duration at variable repetition rates. The dye laser was operated using 4-dicyanomethylene-2-methylene-6(*p*-dimethylaminostyrene)-4H-pyrane (DCM) dye with a tuning range of 610–730 nm. The detection system was a single-photon timing apparatus with a time resolution of 10–20 ps (4). Fluorescence was selected by a double-monochromator with slits set to give a 4-nm bandwidth. A red-sensitive photomultiplier (R955; Hamamatsu Photonics K.K., Hamamatsu City, Japan) with a multialkali photocathode was used for detection. The excitation function had ~120-ps full width at half maximum and 240-ps full width at tenth maximum as measured by single-photon timing with a resolution of ≈10 ps/channel. The high sensitivity of the single-photon timing technique enabled us to use laser pulse intensities for excitation of $<10^{10}$ photons/cm^2 at repetition rates of either 400 or 800 KHz. In general a total fitting range of ≈8 and ≈11 ns has been used in the data evaluation for measurements at the F_0 and F_{max} levels, respectively.

For measurement at the F_0 level the alga suspension was kept in a reservoir with a total volume of 8–12 liters. This large volume was chosen to reduce the influence of the measuring light on the light state of the algae. For the measurements at the F_0 level the algae cells were pumped from the reservoir at a rate of ≈700 ml/min through a flow measuring cuvette of 1.5 × 1.5-mm cross-section with a peristaltic pump to prevent closing of the PS II reaction centers by the measuring light. By using an appropriate length of black tubing we ensured that after leaving the reservoir the algae spent a few seconds in the dark before entering the measuring cuvette. For measurements with closed PS II centers 20 μM 3-(3',4'-dichlorophenyl)-1,1-dimethylurea (DCMU) + 10 mM hydroxylamine were added and the algae were continuously irradiated in the reservoir and in the tubing (for these experiments a transparent tubing was used) with white light of low intensity before being pumped through the measuring cuvette at a low pump rate (≈10 ml/min). For state transitions the whole reservoir was subjected for 30 min to the specific irradiation conditions before the measurement started. During the measurement of a decay-associated spectrum the irradiation conditions in the reservoir were maintained.

All measurements were carried out at ambient temperature (22°–25°C). For inducing a transition to state II the reservoir was irradiated with red fluorescent tubes (Philips TL 20W/15), which have a dominant emission band at 654 nm (light II) (≈0.5 W/m^2). Light I was provided from three slide projectors equipped with either 696-nm interference filters (bandwidth 10 nm; Deutsche Balzers GmbH, Geisenheim, FRG) or, alternatively, with long-pass filters with 50% transmission at 715 nm (RG 9; Schott Optik, Mainz, FRG) with an intensity of 3 W/m^2 to compensate for the reduced absorption at the long wavelengths. For controls the algae were dark-adapted for at least 30 min or the reservoir was subjected to the same white light conditions as were applied in the growth chamber.

Global Data Analysis

For analysis of the decay curves recorded at various emission wavelengths we applied a newly developed deconvolution procedure based on a global optimization algorithm (15, 60). Instead of analyzing individual decay curves recorded at one wavelength all decay curves recorded at different wavelengths are analyzed simultaneously in a single run. The algorithm is based on the assumption that the decay constant (lifetime) of a particular decay component should be independent of wavelength while the preexponential factors (amplitudes) vary. The fluorescence decay $I(t,\lambda)$ is described by a sum of exponential functions

$$I(t,\lambda) = \sum_{i=1}^{n} A_i(\lambda) \exp(-t/\tau_i) . \quad (1)$$

If the lifetimes are independent of emission wavelength the dimensionality of the fitting problem can be reduced from $2 \times N \times n$ to $N \times n + n$ by applying the global analysis. Here, N denotes the number of independent measurements at different wavelengths and n, the number of decay components. The reduction in the number of the free parameters leads to a dramatic improvement both in the accuracy of the extracted parameters as well as in the capability for multicomponent resolution. This latter advantage is important in view of the complexity of the fluorescence decay from photosynthetic tissue (3, 4). The quality of the fits was judged by a global χ^2 value, individual χ^2 values, and plots of the weighted residuals. The iteration procedure applied in our program is a semilinear Marquardt algorithm (61). The feasibility and reliability of the four-exponential analysis has been tested on a number of simulated data sets with three and four decay components, which mimicked the experimental decay-associated spectra. Poissonian noise had been added to these simulated decay data. These tests confirmed the expected drastic improvement of the global data analysis as compared with the conventional single-decay analysis. In all these simulations the theoretical parameters (amplitudes and lifetimes) were recovered very closely, which makes us confident that the present analysis is reliable.

The amplitudes of the decay components obtained from the global analysis procedure were plotted as decay-associated spectra after correction for the wavelength-dependent sensitivity factor of the dectector. The correction factor has been determined as reported previously (4). We like to note that decay-associated spectra obtained in the way described here represent true spectra of individual decay components. Such a decay-associated spectrum should be identical to the spectrum that would be obtained if this component was isolated and then measured individually. This is not to be confused with procedures in which time-resolved spectra are recorded at different delay times after the exciting light pulse (62). In contrast to the former, the latter will in general still represent weighted mixtures of the spectra of all decay components. Again we have preferred to plot the amplitudes of the decay-associated components rather than their yields. Such a plot provides more information since amplitudes are proportional to absorption cross-sections and thus, in turn, to the antenna sizes of the decay components (4). For an individual lifetime component with an exponential decay the relationship between the amplitudes $A(\lambda_{em})$ at excitation wavelength λ_{exc} and emission wavelength λ_{em} and the sample parameters is given by the relationship

$$A(\lambda_{em}) = k_{rad} \cdot \epsilon(\lambda_{exc}) \cdot N \cdot F(\lambda_{em}), \qquad (2)$$

where k_{rad} is the radiative rate constant, $\epsilon(\lambda_{exc})$ the extinction or absorption cross-section at the excitation wavelength, $F(\lambda_{em})$ the shape of the (normalized) fluorescence spectrum, and N the number of Chls contributing to the lifetime component.

Fluorescence Induction Measurements

The fluorescence induction measurements have been carried out on algae cells poisoned with 20 μM DCMU. After adaptation to the desired light state in the way as described above, DCMU was added in the dark and the induction measurement was carried out after a dark time of 2 min. An excitation wavelength of 630 nm (4-nm bandwidth) was used, i.e., the same as in the lifetime measurements, and fluorescence was detected at 682 nm through an interference filter (10-nm bandwidth). The induction kinetics was recorded on a home-built apparatus with a split-time base and analyzed by computer fitting to a function consisting of a sum of a sigmoidal and an exponential component.

RESULTS

Measurement with Open PS II Centers

The decay-associated fluorescence spectra of wild-type *Scenedesmus* have been measured using excitation light of λ_{exc} = 630 nm under four different conditions: (*a*) after

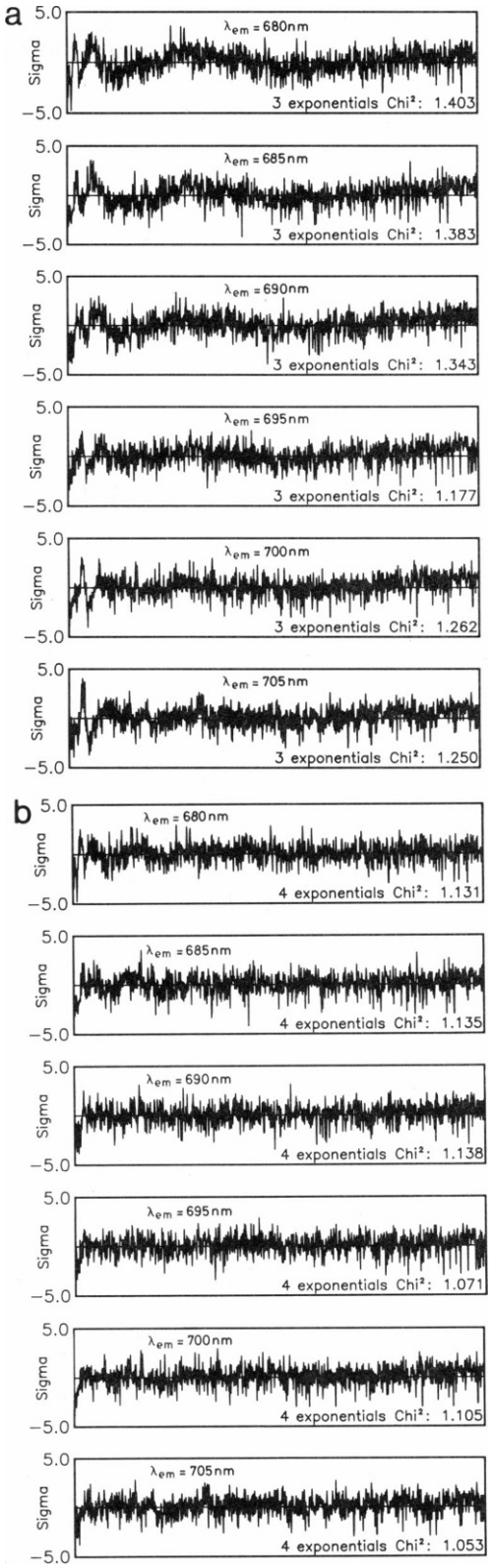

FIGURE 1 Weighted residual plots and χ^2 values of fluorescence decays from a light II–adapted sample of *Scenedesmus* at the F_0 level of fluorescence. The global data analysis procedure has been applied. (*a*) Three-exponential model function; (*b*) four-exponential model function. Note the systematic deviations in the residuals for the three-exponential analysis. The data have been analyzed over a time range of ≈9 ns. (cf. Fig. 2).

irradiation with light I, (*b*) after irradiation using light II, and two controls (*c*) in the dark-adapted state and under (*d*) white light irradiation. Our experimental set-up (see Materials and Methods) enables us to adapt the algae to the above-mentioned light conditions (states) in the reservoir and, independently of these conditions, probe the Chl fluorescence at or very close to the F_0 level. This is possible since the algae are pumped from the reservoir through a flow measuring cuvette and spend <1 ms only in the laser beam (≈1-mm diam) under the pumping conditions used. To obtain data with high signal/noise ratio in reasonable measuring times we concentrated on the wavelength regions where the spectra of the individual decay components show the most pronounced differences. This is the range from ≈680 to 705-nm emission wavelength. Measurements over a wider wavelength range were carried out as well for the purpose of completing the spectra. However, only the data in the middle interval are essential for our conclusions. Fluorescence decays were recorded at 5-nm intervals. In general we could measure three spectra under different irradiation conditions in 1 d from the same sample. We verified that the results were not dependent on the irradiation history of the sample by varying the sequence of irradiations. No influences were found beyond the error limits. Fig. 1, *a* and *b* shows the residual plots and χ^2 values for evaluations of the decay-associated spectra from a light II (λ_{irrad} mostly 654 nm) adapted sample. The deviations in the global three-exponential fit (Fig. 1 *a*) clearly indicate that at least a sum of four exponentials (Fig. 1 *b*) is required for a good fit. For comparison Fig. 2 shows a conventional fit to an individual decay (λ_{em} = 685 nm) taken from the same series. Four-exponential and three-exponential fits are hardly distinguishable in the single decay analysis. This demonstrates the advantages of global data analysis. The differences found in the residuals for this data set in the global analysis is typical of all the other conditions as well.

Figs. 3–5 show the decay-associated spectra obtained under the various irradiation conditions using a four-exponential global analysis in all cases. The same scale applies to Figs. 3–5 since these data have been obtained from the same sample in the sequence presented. All parameters except the irradiation conditions in the reservoir were kept constant. The most pronounced change upon variation of the irradiation conditions occurs in the amplitudes of the components with lifetimes of ≈300 and ≈600 ps (Figs. 3–5). They both have a spectral peak ~685 nm at all conditions. The shorter-lived of these decay components ($\tau \approx 300$ ps) is highest in amplitude in the dark-adapted state and lowest in the light II–adapted state. In contrast the amplitude changes of the other component ($\tau \approx 600$ ps) are in the opposite direction, i.e., maximal amplitude in the light II state and minimal amplitude after dark adaptation. Table I summarizes the lifetimes of the decay components obtained under the different conditions. Both the amplitude and the maximum of the shortest-lived component

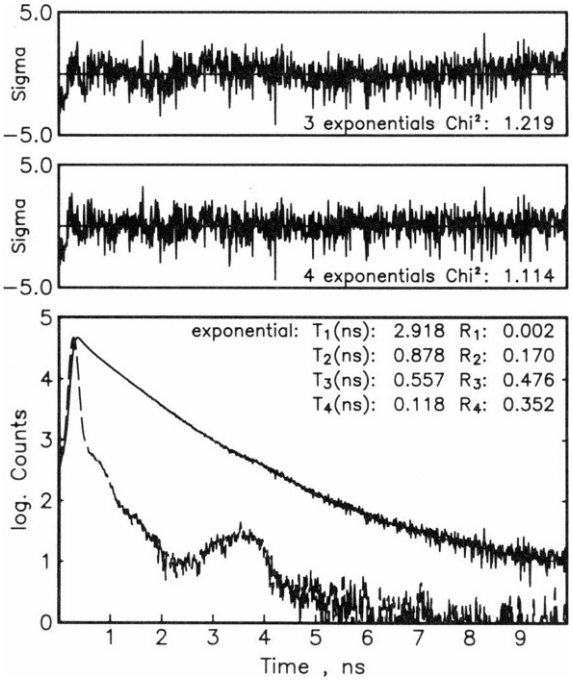

FIGURE 2 Conventional decay analysis at a single wavelength (λ_{em} = 685 nm) for a light II-adapted sample (same data as in Figs. 1 and 4). The residual plots and χ^2 value are given for a three- and a four-exponential model function (*top*). The lower part of the Fig. shows the semilogarithmic presentation of the fluorescence decay (*solid line*) and the excitation function (*dashed line*).

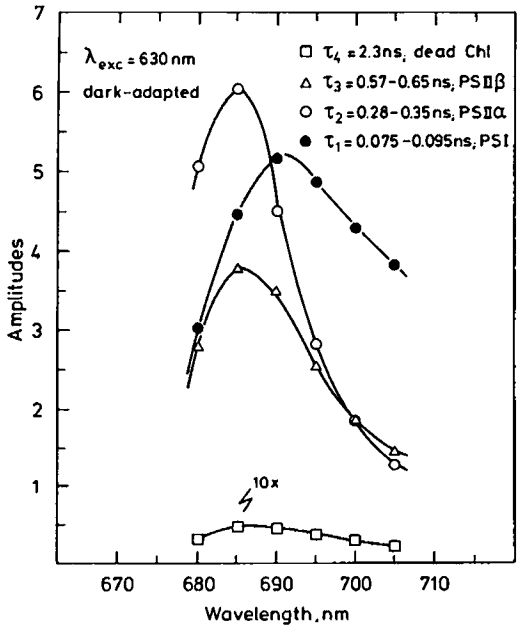

FIGURE 3 Decay-associated fluorescence spectra for dark-adapted cells of *Scendesmus* at the F_0 level of fluorescence (cf. Materials and Methods and first footnote in Table I); λ_{exc} = 630 nm. The spectra have been calculated using the global data analysis procedure. The same scale applies to Figs. 3–5.

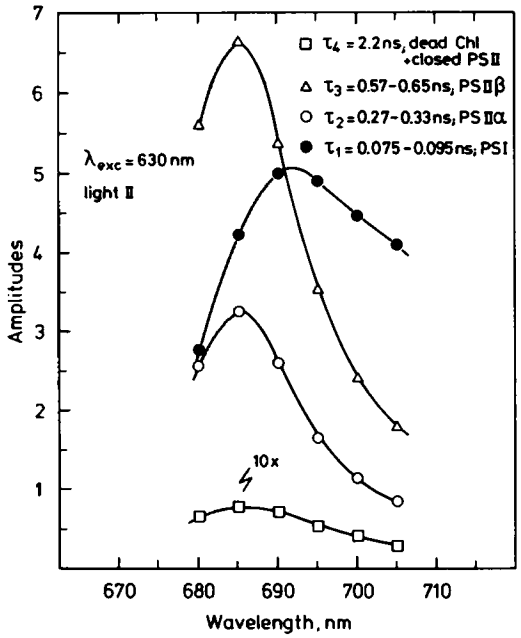

FIGURE 4 Decay-associated fluorescence spectra for light II–adapted cells of *Scendesmus* at the F_0 level of fluorescence (cf. Materials and Methods and first footnote in Table I); λ_{exc} = 630 nm. The spectra have been calculated using the global data analysis procedure. The same scale applies to Figs. 3–5.

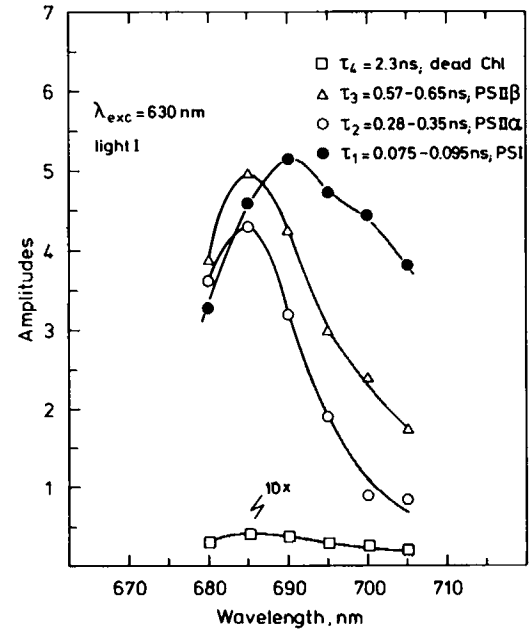

FIGURE 5 Decay-associated fluorescence spectra for light I–adapted cells of *Scenedesmus* at the F_0 level of fluorescence (cf. Materials and Methods and first footnote in Table I); λ_{exc} = 630 nm. The spectra have been calculated using the global data analysis procedure. The same scale applies to Figs. 3–5.

TABLE I
LIFETIMES τ OF THE FLUORESCENCE DECAY COMPONENTS OF *SCENEDESMUS* UNDER VARIOUS CONDITIONS*

	α-Units	β-Units	PS I	τ_{av}, ps‡	ϕ_{total}§
	τ, ps	τ, ps	τ, ps		
Dark-adapted (F_0)	280–350	570–650	75–95	370	1.0
State I (F_0)	280–350	570–650	75–95	370	1.0
State II (F_0)	270–300	590–650	75–95	440	1.19
White light (F_0)	280–350	580–650	75–95	390	1.05
State I (F_{max})	2,200	1,100–1,200	75–95	1450	3.92
State II (F_{max})	2,200	1,100–1,200	75–95	1300	3.51

*The numbers given represent the range of lifetimes found for different samples and independent measurements. Within one sample the lifetimes of the decay components are nearly invariant with respect to state transitions. Only the lifetime for open α-units was generally slightly shorter in state II as compared with the other conditions. The measurement uncertainties are much smaller than the ranges of each lifetime given in the table. The average lifetime τ_{av} and the fluorescence yield ϕ_{total} calculated from the decay-associated spectra are also given.

‡Average lifetime at λ_{em} = 685 nm calculated according to Eq. 3 (data taken from the series presented in Figs. 3–5); the average lifetime is directly proportional to the steady-state fluorescence intensity and yield (see text and Eq. 3).

§Fluorescence yield calculated from the fluorescence decay measurements at λ_{em} = 685 nm. All data are normalized to the yield of dark-adapted algae under F_0 conditions.

($\lambda_{max} \approx$ 690–695 nm, τ = 85 ps) do not depend on the irradiation conditions. Under all conditions a very small amount of a long-lived decay ($\tau \approx$ 2.3 ns, $\lambda_{max} \approx$ 685 nm) is found as well (amplitude < 0.5%). The amplitude of this latter component is neither decreased considerably when the measuring light intensity is reduced nor is it in the dark-adapted state. This behavior excludes closing of PS II reaction centers by the measuring light and points to a very small amount of dead Chl as a cause of this fluorescence component.

Measurements with Closed PS II Centers

The PS II reaction centers have been closed by addition of DCMU and hydroxylamine to a dark-adapted sample and subsequent irradiation with low intensity white light. Under these conditions all PS II reaction centers are closed (F_{max}) and a three-exponential model was sufficient to describe the data in the global analysis procedure (cf. Fig. 6). Fig. 7 shows the decay-associated spectra for the F_{max} condition. The absence of any short-lived decay component other than the one peaking at ≈695 nm at the F_{max} level is particularly noteworthy. We observe two long-lived components with lifetimes of 2.2 and 1.15 ns, which both peak at 685 nm. Their amplitudes are very similar to those found for the 300- and 600-ps components, respectively, at the F_0 level in the dark-adapted state (Fig. 3). All data obtained from the lifetime measurements are compiled in Table I. A full quantitative comparison of the amplitudes with Fig. 3 is not possible, however, since the two measurements have not been carried out on the same sample, and

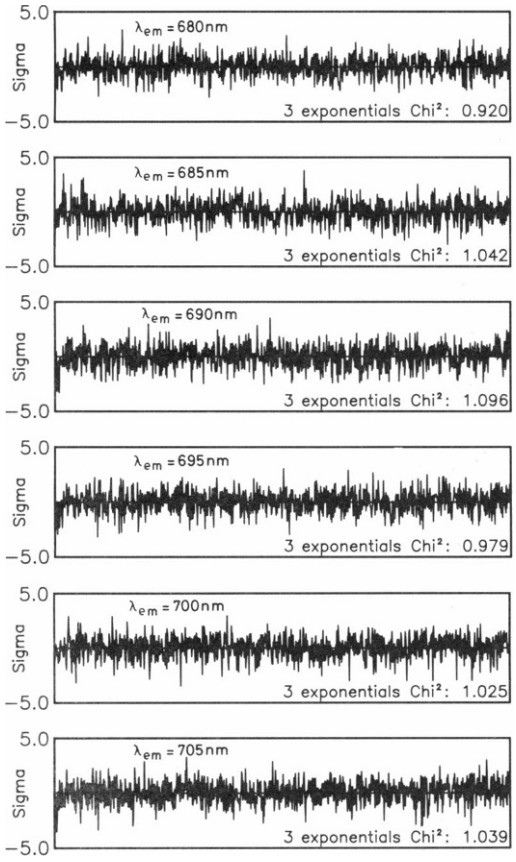

FIGURE 6 Weighted residuals plots and χ^2 values of fluorescence decays from a dark-adapted sample of *Scenedesmus* measured at the F_{max} level of fluorescence (20 μM DCMU + 10 mM hydroxylamine). The global data analysis procedure has been applied. In contrast to the F_0 level a three-exponential model function is sufficient to describe the data at the F_{max} level. The fitting range was ≈11 ns.

slight variations in the relative amplitudes of these components have generally been observed between different samples.

Fluorescence Induction Data

The parameters obtained from the analysis of the fluorescence induction curves of cells adapted to state I or state II are summarized in Table II. The decrease in the ratio of maximum to initial fluorescence (F_{max}/F_0) in state II as compared with state I is typical for state transitions. This decrease is brought about mainly by a decrease in F_{max} but also includes a small increase in the F_0 level. These changes are in good agreement with the corresponding yield calculated from the lifetime measurements at λ_{em} = 685 nm. The rate constant K_β of the slow induction phase is increased by ~20% in state II as compared with its value in state I (3.6 s^{-1}). At the same time the rate constant K_α of the fast phase remained roughly constant (≈18 ± 1 s^{-1}).

DISCUSSION

During recent years a number of low intensity picosecond fluorescence studies have been carried out on a large

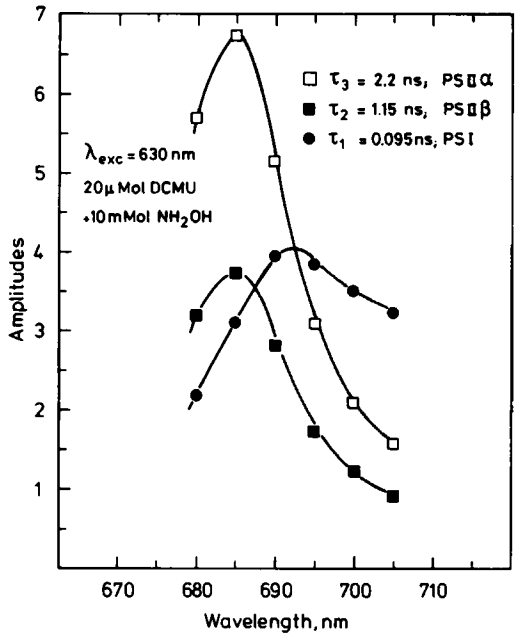

FIGURE 7 Decay-associated fluorescence spectra of dark-adapted cells (λ_{exc} = 630 nm) of *Scendesmus* at the F_{max} level of fluorescence (20 μmol DCMU and 10 mmol hydroxylamine added); same data as in Fig. 6. The spectra have been calculated using the global data analysis procedure.

variety of photosynthetic tissue involving both higher plant chloroplasts and green algae. It has been found in all of these studies that three exponential functions were necessary to describe the Chl fluorescence decay (7–13, 63–67). Based on an extended study of decay-associated excitation and emission spectra, we have argued very recently that four exponentials were necessary to describe the fluorescence decay of *Chlorella vulgaris* in general (3, 4). This result is supported by the global data analysis technique. The data presented in Figs. 1–7 both demonstrate the potential of the global data analysis procedure and reinforce the evidence for the need of generally four exponentials to describe the decay curves of cells with open PS II

TABLE II
COMPARISON OF FLUORESCENCE INDUCTION DATA OF DCMU-INHIBITED *SCENEDESMUS* CELLS IN STATE I AND STATE II WITH CORRESPONDING DATA CALCULATED FROM DECAY-ASSOCIATED SPECTRA

	F_0*	F_{max}/F_0‡	K_β§	ϕ_{max}/ϕ_0‖	P¶
			s^{-1}		
State I	4.9	3.4	3.6	3.9	0.50
State II	5.3	2.9	4.3	3.0	0.45

*Initial (F_0) value from fluorescence induction experiments.
‡Ratio of maximum to initial fluorescence yield in fluorescence induction experiment with DCMU-treated cells (20 μmol DCMU).
§Rate constant of the slow induction phase.
‖Ratio of maximum to minimum fluorescence yield from fluorescence lifetime experiments calculated from ϕ_{total} data in Table I. The cells were treated with both DCMU and hydroxylamine (for conditions see Fig. 7).
¶Connectivity parameter determined from fluorescence induction according to reference 78.

centers. However, since the long-lived fourth component of low amplitude arises from a small amount of dead Chl we shall omit it in further discussions. Nevertheless it has to be taken into account in the data analysis since there an omission would give rise to erroneous results for the lifetimes of the other components. As compared with single decay analysis used in previous work the spectra (amplitudes) and lifetimes are determined with better precision using the global analysis approach.

At the F_0 level we find a very fast component ($\tau_1 = 85 \pm 10$ ps) with an emission maximum slightly below 700 nm, which is red-shifted as compared with the other three spectra. In addition we find a fast ($\tau_2 \approx 300$ ps) and an intermediate ($\tau_3 \approx 600$ ps) component with appreciable amplitudes at the F_0 level. Both of these lifetimes are somewhat longer than the corresponding components in *Chlorella* (3, 4). Their spectra with maxima at ≈685 nm are very similar to those of *Chlorella*. The almost invariant lifetimes of all components found under the various conditions within a series are indicative of the fact that under our conditions we indeed probe the F_0 level. This is of particular importance for the light-adapted conditions.

The lifetimes and amplitudes of both the τ_2 and τ_3 components at F_0 seem to depend somewhat on the growth conditions. We also found that generally the τ_2 component at the F_0 level was ≈10% shorter-lived in state II as compared with the other conditions. This slight variation is probably related to the variation in the antenna size of that component. In contrast the lifetimes τ_1 and τ_4 are largely invariant under the different adaptations. Under all the conditions studied (different samples, different irradiation) the lifetime τ_1 did not vary by more than ±10 ps, which is the experimental uncertainty.

PS I Fluorescence

Previously (3, 4) a short-lived component with lifetime $\tau_1 \approx$ 80 ps was assigned to arise from PS I on the basis of its red-shifted emission spectrum as compared with the other components, its insensitivity to the state of PS II reaction centers, and its preferential excitation at long wavelength. The shortest-lived component found here in *Scenedesmus* has very similar properties. The measurements at the F_{max} level show that its lifetime and spectral shape do not depend on the state of the PS II centers. In analogy to previous studies (3, 4, 62), we therefore assign the fast ($\tau_1 \approx 85$ ps) component again to PS I.

It is important to note that under the various irradiation conditions, i.e., light I, light II, white light, and dark-adapted state, we do not observe a significant change in either the maximum amplitude, the spectral shape, or the lifetime of the $\tau_1 = 85$ ps component. Provided there should be any changes in cross-section (amplitude) at all, we are confident that they are about an order of magnitude smaller than those observed in the other decay components. In fact our data indicate that the amplitude of the PS I component changes by <5% under the various irradiation conditions used for state transitions. This is an important result since the amplitude of a kinetic component in the decay-associated spectra is a measure of the antenna size and/or absorption cross-section of those units giving rise to that kinetic component (see Eq. 2). We can thus exclude a significant variation of the PS I absorption cross-section or antenna size by direct attachment or detachment of LHCP to/from PS I in response to state transitions. A mechanism involving the attachment of LHCP to PS I has been proposed by several groups to explain the results of both state transitions as well as in vitro thylakoid phosphorylation (36, 37, 40, 41, 68–70).

PS II Fluorescence

The experiments with inhibitors of PS II show that the τ_2 and τ_3 components at F_0 and F_{max} both originate from PS II in agreement with earlier work (4, 7, 11). We assume that the antenna size of PS II remains unchanged when the PS II reaction centers are closed. Since the amplitude in the decay-associated spectrum is a measure of the antenna size (see above), a comparison of the amplitudes of the various kinetic components in completely closed PS II reaction centers (DCMU + hydroxylamine) on the one hand with the F_0 data on the other hand should reveal those components arising from the same pigment bed(s) at the two extreme fluorescence levels. On this basis it is easily seen from our decay-associated spectra that the 300- and 600-ps decay components at the F_0 level turn into fluorescence decays with lifetimes of 2.2 and 1.2 ns, respectively, at the F_{max} level.

Our data prove that at fully closed PS II centers the 300- and 600-ps components, which are characteristic of open PS II centers, both disappear. We have suggested such a behavior already from our earlier data (4, 11, 12). The use of the global data analysis technique makes this result now even more evident. This finding is of considerable importance for an understanding of the exciton trapping and charge separation kinetics in PS II (71). We can now conclude also more reliably that each of the three different units, i.e., PS I, PS IIα, and PS IIβ, gives rise to a fluorescence decay that is each close to a single exponential. No separate fluorescence emission from LHCP II is observed under any of the conditions examined. The latter finding is indicative of a tight coupling of LHCP II to the PS II core antennae. This conclusion has also been drawn by Berens et al. (72).

Comparison with Other Data and Interpretations

Hodges and Moya (56) have recently criticized the assignment of the two PS II fluorescence decay components to PS II α- and β-units. In contrast to our interpretation (4) they claim that the long-lived PS II component at F_0 ($\tau = 450$–600 ps) turns into the long-lived PS II component ($\tau \geq 2.2$ ns) at F_{max}. Correspondingly the short-lived PS II component at F_0 ($\tau \approx 200$ ps) should turn into the

middle component ($\tau \approx 1.4$ ns) at F_{max}. They also claim a proportionality between the yield and the lifetime for each of the two variable lifetime components upon closing PS II centers. Such a proportionality would require a constant amplitude for each of the variable components due to the basic relationship given in Eq. 3. However, this constancy of the amplitudes is not present in their data (56). For example for *Chlorella pyrenoidosa* the amplitude of the 450-ps component at F_0 and the claimed corresponding component of 2.6 ns at F_{max} have amplitudes of 44 and 20%, respectively. A similarly drastic variation from 44 to 74% was found for the 220-ps (F_0) and the claimed corresponding 1.44-ns component (F_{max}). Large changes in the amplitude, albeit in the opposite direction, were observed for spinach chloroplasts upon closing PS II centers (56). Furthermore they report a drastic decrease from $\approx$10 to $\leq$2% in the relative amplitudes of the shortest-lived (PS I) component in all cases when going from F_0 to F_{max}. All of these amplitude changes are in clear contradiction to their claimed proportionality between lifetime and yield of the individual components.

The interpretation and assignments proposed in reference 56 additionally create a number of contradictions with data and kinetic models in the literature (4, 65, 72, 73). The proposed correspondence between the 600-ps component (F_0) and the $\geq$2.2-ns component (F_{max}) and their assignment to reexcited LHCP would imply a rather inefficient coupling of LHCP to the PS II core antenna, which would be inconsistent with an efficient functioning of the LHCP complex (2, 4, 65, 72).

The interpretation of Hodges and Moya represents a slightly modified version of the well-known tripartite model originally proposed by Butler (74) but later recognized as inadequate for the interpretation of the lifetime data (4, 72, 73). While the kinetic equations describing the tripartite model predicts indeed a biexponential decay kinetics for PS II, at least at the extreme stages F_0 and F_{max}, they also predict that any change in lifetime due to closing of reaction centers will result also in changes of the relative amplitudes of these components (72), in contrast to the interpretation of reference 56. Likewise changes in the relative amplitudes of the kinetic components in response to, e.g., state transitions, as presented in this work, without concomitant changes in the lifetimes would also be inconsistent with the kinetic equations describing the tripartite model. The assignment of kinetic components in reference (56) ignores this fundamental coupling between amplitudes and lifetimes of kinetic components, which is characteristic for the tripartite model.

In contrast, an assignment of the kinetic components in terms of two different types of PS II units results in an agreement between the experimental data and the corresponding kinetic equations (4, 65, 72). Such a heterogeneous model can explain a wide range of lifetime data, including the effects of state transitions, closing of PS II reaction centers (4, 65), as well as the decay-associated excitation spectra of the different components (4). Thus, despite some controversial reports in the literature on the proposed properties of PS II α- and β-units, our working hypothesis is to relate the observed PS II heterogeneity in the fluorescence kinetics to α- and β-centers. In this context it is gratifying to see that the changes in fluorescence induction data (cf. Table II), which have been used in the past to probe α,β-heterogeneity, agree well with the corresponding data obtained from the lifetime measurements.

State Transitions and α,β-Heterogeneity

A controversy has arisen in the past whether the dark-adapted state in various organisms is state I or state II (16, 17, 19, 21, 25, 75). We have observed pronounced variations in the amplitudes of the two decay components associated with lifetimes of $\approx$300 (τ_2) and 600 ps (τ_3), respectively, at the F_0 level. The most extreme opposite states are obtained in the dark-adapted vs. the light II–adapted sample. Under these conditions the amplitudes of the components τ_2 and τ_3 are approximately reversed at the F_0 level. Light II irradiation strongly favors the τ_3 component, whereas dark adaption increases the amplitude of τ_2 and concomitantly decreases that of τ_3. Judged on the basis of the decay-associated spectra the dark-adapted state is closer to the light I state (state I). This observation sheds light onto contradictory reports as to whether the dark-adapted state is state I or state II in *Scenedesmus*. The terminology has been introduced originally to designate the two extremes (16). If the terms are applied in this sense the dark-adapted state should perhaps be termed an extreme state I whereas the light II adapted state represents the other extreme (state II). This is consistent with the findings and notion of Bonaventura and Myers (16), but in contrast to other reports (19, 21).

It is well-known from fluorescence induction measurements that the F_{max} level of fluorescence and the amount of F_{var} are sensitive to state transitions. Both of them are considerably lower in the light II–adapted state (19–22, 30). In contrast to that, the reported variations in the F_0 level have been much smaller (19–21, 30) (a slight decrease has often been observed) or even absent (22). At first sight, the large variations in amplitudes (and yields) at F_0 observed here might thus come as a surprise. However, steady-state spectroscopy and fluorescence induction starting from the F_0 level cannot distinguish between the various decay components. We can get a good estimate, however, of what would be expected under similar conditions in a steady-state measurement by calculating the average fluorescence lifetimes τ_{av} and the relative fluorescence quantum yields from the decay-associated spectra.

$$\sum_i A_i\tau_i = \sum_i \phi_i = \phi_{total}$$

$$\tau_{av} = \frac{\Sigma_i A_i\tau_i}{\Sigma A_i} = \frac{\Sigma_i \phi_i}{\Sigma A_i}. \qquad (3)$$

In these formulae the A_i are the amplitudes of the decay-associated spectra, τ_i the lifetimes, and ϕ_i the fluorescence yields of component *i*.

These data are given in Table I for λ_{em} = 685 nm and λ_{exc} = 630, a situation that is typical of many fluorescence induction experiments reported in the literature (τ_{av} will depend on the excitation wavelength). The values of τ_{av} and the fluorescence yield ϕ_{total} are shown in Table I for the various irradiation conditions. They are directly proportional to the expected stationary F_0 levels of fluorescence. Our data indicate a slightly smaller F_0 level in the dark-adapted and light I–adapted states (state I) as compared with the light II–adapted state. The difference is 10–20% and thus should be detectable in fluorescence induction experiments. This expectation is indeed in agreement with our induction data given in Table II. In state II the F_{max}/F_0 ratio is reduced mostly due to a reduced F_{max} value, but also due to a small increase in F_0. This finding is reminiscent of the situation upon phosphorylation of thylakoids reported by Kyle et al. (76). Also at the F_{max} level our results from the fluorescence decay measurements agree well with those from the fluorescence induction measurements (Table II). In agreement with other groups (19–22, 30) we also find a decrease of the F_{max} fluorescence yield in state II. By extrapolation this decrease can now be related to an increased contribution (amplitude) of the $\tau_2 \approx$ 1.2-ns decay component and a concomitant decrease in the amplitude of the 2.1-ns component at F_{max} in state II as compared with state I.

Reorganization of PS II Antenna

Our data indicate that state transitions do not reversibly induce or remove new lifetime components either at the F_0 level or at F_{max}. More specifically, we do not find a decay component with a lifetime characteristic of uncoupled LHCP. The changes in lifetime of individual components in response to state transitions, as shown in Table I, are small or even negligible in most cases. We can thus exclude models that involve the mere uncoupling of LHCP as a mechanism to reduce PS II activity upon transition to state II. The spectra and lifetimes of the τ_3 and τ_2 components found here and in our previous work (4) would not be consistent with such an interpretation. Instead our data suggest opposite changes in the total absorption cross-sections associated with the two types of PS II units. These components are, with varying amounts, present under all conditions. Thus in state II, the total absorption cross-section of those units with a lifetime of ~600 ps is at a maximum and that of the fast PS II units is at a minimum. In state I (dark-adapted state or light I) this distribution is reversed. The total PS II absorption cross-section ($\alpha + \beta$—units, i.e., sum of the PS II amplitudes) is invariant to state transitions within the experimental error, as can be deduced from their amplitudes in Figs. 3–5. It is particularly noteworthy that the sum of the amplitudes (at 685 nm) of all PS II decay components is constant within better than 5% in a series both in response to state transitions (Figs. 3–5) and upon closing PS II centers (Fig. 7). This finding is also in full agreement with the invariance of the PS I antenna size (see above) and excludes a direct redistribution of antennae pigments in favor of PS I of vice versa. Our results are, in principle, in line with recent findings that phosphorylation reversibly increases the amount or antenna size of β-units and decreases the amount or antenna size of α-units (76, 77). Within this model all our data can be reconciled easily with the results of reference 76.

To explain the large observed variations in the amplitudes of the τ_2 and τ_3 components in response to state transitions we propose as a working hypothesis a model of the antenna organization in which the basic regulation mechanism in a transition to state II involves a reversible phosphorylation and subsequent migration of LHCP from α- to β-units. The attachment of phosphorylated LHCP to β-centers increases their absorption cross-section, which explains also the increase in the rate constant of the slow fluorescence induction component in state II (cf. Table II). A schematic diagram of this model is given in Fig. 8.

Our experiments present a critical test of the hypothesis that state transitions should alter the direct absorption cross-section of PS I by an attachment of LHCP II to this photosystem. A minor contribution of this mechanism cannot be excluded. We can exclude, however, that the direct attachment of LHCP to PS I antennae provides the major effect of a transition to state II. We conclude that the regulation mechanism operative in state transitions

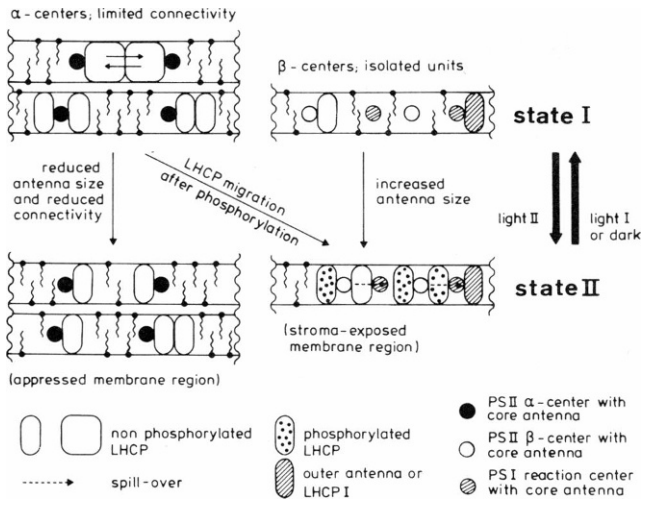

FIGURE 8 Schematic model of the PS II antennae organization in states I and II. Note that the absolute number of α- and β-centers is constant in the two states. PS I is concentrated in the thylakoid regions where β-centers are located (stroma-exposed thylakoids). The regulation mechanism is based on the reversible migration of phosphorylated LHCP from α-centers to β-centers. The model also indicates that up to 30% of the total Chl in PS II (referred to the total absorption cross-section of PS II at 630 nm) may be mobile. Phosphorylated LHCP does not attach directly to PS I (see also reference 79).

primarily affects the cross-sections of the two different PS II units only, which are best characterized in terms of α,β-heterogeneity so far. The direct antenna size of PS I remains unchanged in the state transition. There could occur indirect variations in the effective antenna sizes by a spill-over mechanism, however. The full discussion of the model of the antenna organization including the quantitative analysis of spill-over effects is beyond the scope of this report and will therefore be provided in a forthcoming paper.

The decay-associated fluorescence spectra provided further evidence in support of the α,β-heterogeneity of PS II reaction centers. We interpret the lifetimes of $\approx$300 and $\approx$600 ps in open PS II α- and β-units, respectively, as overall trapping times of excitons in the complete antennae, including both the core Chl and LHCP. Our data suggest functional and structural differences between the two types of PS II centers. Methods other than fluorescence spectroscopy will have to be applied to gain more insight into the structural properties of β-units.

We thank Professor K. Schaffner for generous support and interest in this work. Miss S. Hermann, Mr. K. Kerpen, and Mr. U. Pieper provided able technical assistance. We also thank Mr. H. Brock for help with the laser system and Mr. Stempfle for support in the programming of the global data analysis routine.

Partial financial support from the Deutsche Forschungsgemeinschaft is gratefully acknowledged. A starting culture of *Scenedesmus* has been kindly provided by the group of Professor H. Senger, Marburg.

Received for publication 12 May 1986 and in final form 18 June 1987.

REFERENCES

1. Karukstis, K. K., and K. Sauer. 1983. Fluorescence decay kinetics of chlorophyll in photosynthetic membranes. *J. Cell. Biochem.* 23:131–158.
2. Holzwarth, A. R. 1986. Fluorescence lifetimes in photosynthetic systems. *Photochem. Photobiol.* 43:707–725.
3. Wendler, J., W. Haehnel, and A. R. Holzwarth. 1984. Time-resolved picosecond fluorescence spectra of the antenna chlorophylls in the green alga Chlorella vulgaris. *In* Ultrafast Phenomena IV. D. H. Auston and K. B. Eisenthal, editors. Springer-Verlag, Berlin, Heidelberg. 38:503–505.
4. Holzwarth, A. R., J. Wendler, and W. Haehnel. 1985. Time-resolved picosecond fluorescence spectra of the antenna chlorophylls in Chlorella vulgaris. Resolution of PS I fluorescence. *Biochim. Biophys. Acta.* 807:155–167.
5. Haworth, P., K. K. Karukstis, and K. Sauer. 1983. Picosecond fluorescence kinetics in spinach chloroplasts at room temperature. Effects of phosphorylation. *Biochim. Biophys. Acta.* 725:161–271.
6. Karukstis, K. K., and K. Sauer. 1983. Potentiometric titration of photosystem II fluorescence decay kinetics in spinach chloroplasts. *Biochim. Biophys. Acta.* 722:364–371.
7. Haehnel, W., J. A. Nairn, P. Reisberg, and K. Sauer. 1982. Picosecond fluorescence kinetics and energy transfer in chloroplasts and algae. *Biochim. Biophys. Acta.* 680:161–173.
8. Magde, D., S. J. Berens, and W. L. Butler. 1982. Picosecond fluorescence in spinach chloroplasts. *Proc. Soc. Photo. Opt. Instrum. Eng.* 322:80–86.
9. Gulotty, R. J., G. R. Fleming, and R. S. Alberte. 1982. Low-intensity picosecond fluorescence kinetics and excitation dynamics in barley chloroplasts. *Biochim. Biophys. Acta.* 682:322–331.
10. Nairn, J. A., W. Haehnel, P. Reisberg, and K. Sauer. 1982. Picosecond fluorescence kinetics in spinach chloroplasts at room temperature. Effects of Mg^{2+}. *Biochim. Biophys. Acta.* 682:420–429.
11. Haehnel, W., A. R. Holzwarth, and J. Wendler. 1983. Picosecond fluorescence kinetics and energy transfer in the antenna chlorophylls of green algae. *Photochem. Photobiol.* 37:435–443.
12. Holzwarth, A. R., W. Haehnel, J. Wendler, G. W. Suter, and R. Ratajczak. 1984. Picosecond fluorescence kinetics and energy transfer in antennae chlorophylls of green algae and membrane fractions of thylakoids. *In* Advances in Photosynthesis Research. Vol. 1. C. Sybesma, editor. Nijhoff/Junk, The Hague. 73–76.
13. Berens, S. J. 1984. Picosecond fluorescence in spinach chloroplasts. Ph.D. Thesis. University of California, San Diego. 121 pp.
14. Knorr, F. J., and J. M. Harris. 1981. Resolution of multicomponent fluorescence spectra by an emission wavelength-decay time data matrix. *Anal. Chem.* 53:272–276.
15. Knutson, J. R., J. M. Beechem, and L. Brand. 1983. Simultaneous analysis of multiple fluorescence decay curves: a global approach. *Chem. Phys. Lett.* 102:501–507.
16. Bonaventura, C., and J. Myers. 1969. Fluorescence and oxygen evolution from Chlorella pyrenoidosa. *Biochim. Biophys. Acta.* 189:366–383.
17. Murata, N. 1969. Control of excitation transfer in photosynthesis. I. Light-induced change of chlorophyll a fluorescence in Porphyridium cruentum. *Biochim. Biophys. Acta.* 172:242–251.
18. Allen, J. F. 1983. Regulation of photosynthetic phosphorylation. *CRC Crit. Rev. Plant. Sci.* 1:1–22.
19. Sane, P.V., D. Furtado, T.S. Desai, and V.G. Tatake. 1982. A study of state changes in Chlorella: the effect of uncoupler and energy transfer inhibitors. *Z. Naturforsch. Sect. C. Biosci.* 37c:458–463.
20. Hodges, M., and J. Barber. 1983. State 1-state 2 transitions in a unicellular green algae. Analysis of invivo chlorophyll fluorescence induction curves in the presence of 3-(3,4-dichlorophenyl)-1,1-dimethylurea (DCMU). *Plant Physiol.* 72:1119–1122.
21. Satoh, K., and D.C. Fork. 1983. State I-state II transitions in the green alga Scenedesmus obliquus. *Photochem. Photobiol.* 37:429–434.
22. Saito, K., W.P. Williams, J.F. Allen, and J. Bennett. 1983. Comparison of ATP-induced and state 1/state 2-related changes in excitation energy distribution in Chlorella vulgaris. *Biochim. Biophys. Acta.* 724:94–103.
23. Butko, P. 1984. Changes in photosynthetic apparatus and excitation energy distribution in Chlorella during the life cycle. *Photobiochem. Photobiophys.* 8:63–72.
24. Telfer, A., and J. Barber. 1981. ATP-dependent state-1 state-2 changes in isolated pea thylakoids. *FEBS (Fed. Eur. Biochem. Soc.) Lett.* 129:161–165.
25. Satoh, K., and D. C. Fork. 1983. Changes in the distribution of light energy between the two photosystems in spinach leaves. *Photosyn. Res.* 4:71–79.
26. Hodges, M., and J. Barber. 1983. Photosynthetic adaptation of pea plants grown at different light intensities: State 1-State 2 transitions and associated chlorophyll fluorescence changes. *Planta.* 157:166–173.
27. Telfer, A., J. F. Allen, J. Barber, and J. Bennett. 1983. Thylakoid protein phosphorylation during state-1 state-2 transitions in osmotically shocked pea chloroplasts. *Biochim. Biophys. Acta.* 722:176–181.
28. Canaani, O., D. Cahen, and S. Malkin. 1982. Photosynthetic chromatic transitions and Emerson enhancement effects in intact leaves studied by photoacoustics. *FEBS (Fed. Eur. Biochem. Soc.) Lett.* 150:142–146.
29. Canaani, O., J. Barber, and S. Malkin. 1984. Evidence that phosphorylation and dephosphorylation regulate the distribution of excita-

tion energy between the two photosystems of photosynthesis in vivo: photoacoustic and fluorimetric study of an intact leaf. *Proc. Natl. Acad. Sci. USA.* 81:1614–1618.

30. Wollman, F.-A., and P. Delepelaire. 1984. Correlation between changes in light energy distribution and changes in thylakoid membrane polypeptide phosphorylation in Chlamydomonas reinhardtii. *J. Cell Biol.* 98:1–7.
31. Horton, P., and M. T. Black. 1983. A comparison between cation and protein phosphorylation effects on the fluorescence induced curve in chloroplasts treated with 3-(3,4-dichlorphenyl)-1,1-dimethylurea. *Biochim. Biophys. Acta.* 722:214–218.
32. Horton, P., and M. T. Black. 1980. Activation of adenosine 5'triphosphate-induced quenching of chlorophyll fluorescence by reduced plastoquinone. The basis of state I-state II transitions in chloroplasts. *FEBS (Fed. Eur. Biochem. Soc.) Lett.* 119:141–144.
33. Bennett, J. 1979. Chloroplast phosphoproteins. The protein kinase of thylakoid membranes is light-dependent. *FEBS (Fed. Eur. Biochem. Soc.) Lett.* 103:342–344.
34. Bennett, J., K. E. Steinback, and C. J. Arntzen. 1980. Chloroplast phosphoproteins: regulation of excitation energy transfer by phosphorylation of thylakoid membrane polypeptides. *Proc. Natl. Acad. Sci. USA.* 77:5253–5257.
35. Steinback, K. E., S. Bose, and D. J. Kyle. 1982. Phosphorylation of the light-harvesting chlorophyll-protein regulates excitation energy distribution between photosystem II and photosystem I. *Arch. Biochem. Biophys.* 216:356–361.
36. Haworth, P., D. J. Kyle, P. Horton, and C. J. Arntzen. 1982. Chloroplast membrane protein phosphorylation. *Photochem. Photobiol. 36:743–748.*
37. Barber, J. 1983. Membrane conformational changes due to phosphorylation and the control of energy transfer in photosynthesis. *Photobiochem Photobiophys.* 5:181–190.
38. Barber, J. 1983. Photosynthetic electron transport in relation to thylakoid membrane composition and organization. *Plant Cell Eviron.* 6:311–322.
39. Ley, A. C., and W. L. Butler. 1980. Energy distribution in the photochemical apparatus of Porphyridium cruentum in state I, and state II. *Biochim. Biophys. Acta.* 592:349–363.
40. Kyle, D. J., L. A. Staehelin, and C. J. Arntzen. 1983. Lateral mobility of the light-harvesting complex in chloroplast membranes control excitation energy distribution in higher plants. *Arch. Biochem. Biophys.* 222:527–541.
41. Staehelin, L. A., and C. J. Arntzen. 1983. Regulation of chloroplast membrane function: Protein phosphorylation changes the spatial organization of membrane components. *J. Cell Biol.* 97:1327–1337.
42. Torti, F., P. D. Gerola, and R. C. Jennings. 1984. Membrane phosphorylation leads to the partial detachment of the chlorophyll a/b protein from photosystem II. *Biochim Biophys. Acta.* 767:321–325.
43. Melis, A., and P. H. Homann. 1975. Kinetic analysis of the fluorescence induction in 3-(3,4-dichlorophenyl)-1,1-dimethylurea poisoned chloroplasts. *Photochem. Photobiol.* 21:431–437.
44. Melis, A., and P. H. Homann. Heterogeneity of the photochemical centers in system II of chloroplast. *Photochem. Photobiol.* 23:343–350.
45. Melis, A., and A. P. G. M. Thielen. 1980. The relative absorption cross-sections of photosystem I and photosystem II in chloroplasts from three types of Nicotiana tabacum. *Biochim. Biophys. Acta.* 589:275–286.
46. Thielen, A. P. G. M., and H. J. van Gorkom. 1981. Quantum efficiency and antenna size of photosystem II alpha, photosystem II beta and photosystem I in tobacco chloroplasts. *Biochim. Biophys. Acta.* 635:111–120.
47. Melis, A., and J. M. Anderson. 1983. Structural and functional organization of the photosystem in spinach chloroplasts. Antenna size, relative electron-transport capacity, and, chlorophyll composition. *Biochim. Biophys. Acta.* 724:473–484.
48. Melis, A. 1978. Oxidation-reduction potential dependence of the two kinetic components in chloroplast system 2 primary photochemistry. *FEBS (Fed. Eur. Biochem. Soc.) Lett.* 95:202–206.
49. Melis, A., and L. N. M. Duysens. 1979. Biphasic energy conversion kinetics and absorbance difference spectra of photosystem II of chloroplasts. Evidence for two different photosystem II reaction centers. *Photochem. Photobiol.* 29:373–382.
50. Thielen, A. P. G. M., and H. J. van Gorkom. 1981. Energy transfer and quantum yield in photosystem II. *Biochim. Biophys. Acta.* 637:439–446.
51. Thielen, A. P. G. M., and H. J. van Gorkom. 1981. Redox potentials of electron acceptors in photosystem II-alpha and II-beta. *FEBS (Fed. Eur. Biochem. Soc.) Lett.* 129:205–209.
52. Horton, P., and E. Croze. 1979. Characterization of two quenchers of chlorophyll fluorescence with different midpoint oxidation-reduction potentials in chloroplasts. *Biochim. Biophys. Acta.* 545:188–201.
53. Anderson, J. M., and A. Melis. 1983. Localization of different photosystems in separate regions of chloroplast membranes. *Proc. Natl. Acad. Sci. USA.* 80:745–749.
54. Anderson, J. M., and A. Melis. 1983. Lateral organization of photosystem I, photosytem II alpha and photosystem II beta in spinach-chloroplasts. *Proc. Aust. Biochem. Soc.* 15:99–99.
55. Hodges, M., and J. Barber. 1986. Analysis of chlorophyll fluorescence induction kinetics exhibited by DCMU-inhibited thylakoids and the origin of alpha and beta centers. *Biochim. Biophys. Acta.* 848:239–246.
56. Hodges, M., and I. Moya. 1986. Time-resolved chlorophyll fluorescence studies of photosynthetic membranes: resolution and characterization of four kinetic components. *Biochim. Biophys. Acta.* 849:193–202.
57. Bishop, N. I., and H. Senger. 1971. Preparation and photosynthetic properties of synchronous cultures of Scenedesmus. *Methods Enzymol.* 23:53–66.
58. Holden, M. 1965. Chlorophylls. *In* Chemistry and Biochemistry of Plant Pigments. T.W. Goodwin, editor. Academic Press, London. 461–488.
59. MacKinney, G. 1941. Absorption of light by chlorophyll solutions. *J. Biol. Chem.* 140:315–322.
60. Holzwarth, A. R., J. Wendler, and G. W. Suter. 1987. Studies on chromophore coupling in isolated phycobiliproteins. II. Picosecond energy transfer kinetics and time-resolved fluorescence spectra of C-Phycocyanin from Synechococcus 6301 as a function of the aggregation state. *Biophys. J.* 51:1–12.
61. Marquardt, D. W. 1963. An algorithm for least-squares estimation of nonlinear parameters. *J. Soc. Ind. Appl. Math.* 11:431–441.
62. Yamazaki, I., M. Mimuro, N. Tamai, T. Yamazaki, and Y. Fujita. 1985. Picosecond time-resolved fluorescence spectra of photosystem I and II in Chlorella pyrenoidosa. *FEBS (Fed. Eur. Biochem. Soc.) Lett.* 179:65–68.
63. Karukstis, K. K., and K. Sauer. 1983. Picosecond fluorescence kinetics studies of electron acceptor q redox heterogeneity. *Biochim. Biophys. Acta.* 725:246–253.
64. Fleming, G. R., W. T. Lotshaw, R. J. Gulotty, M. C. Chang, and J. W. Petrich. 1983. Picosecond spectroscopy of solutions, proteins and photosynthetic membranes. *Laser Chem.* 3:181–201.
65. Berens, S. J., J. Scheele, W. L. Butler, and D. Magde. 1985. Time-resolved fluorescence studies of spinach chloroplasts. Evidence for the heterogeneous bipartite model. *Photochem. Photobiol.* 42:51–57.
66. Moya, I., M. Hodges, and J.-C. Barbet. 1986. Modification of room-temperature picosecond chlorophyll fluorescence kinetics in green algae by photosystem II trap closure. *FEBS (Fed. Eur. Biochem. Soc.) Lett.* 198:256–262.
67. Gulotty, R. J., L. Mets, R. S. Alberte, and G. R. Fleming. 1985.

Picosecond fluorescence study of photosynthetic mutants of Chlamydomonas reinhardii: origin of the fluorescence decay kinetics of chloroplasts. *Photochem. Photobiol.* 41:487–496.

68. Haworth, P., D. J. Kyle, and C. J. Arntzen. 1982. A demonstration of the physiological role of membrane phosphorylation in chloroplasts, using the bipartite and tripartite models of photosynthesis. *Biochim. Biophys. Acta.* 680:343–351.
69. Telfer, A., M. Hodges, P. A. Millner, and J. Barber. 1984. The cation-dependence of the degree of protein phosphorylation-induced unstacking of pea thylakoids *Biochim. Biophys. Acta.* 766:554–562.
70. Kyle, D.J., T.-Y. Kuang, J. L. Watson, and C. J. Arntzen. 1984. Movement of a sub-population of the light harvesting complex (LHCII) from grana to stroma lamellae as a consequence of its phosphorylation. *Biochim. Biophys. Acta.* 765:89–96.
71. Schatz, G. H., and A. R. Holzwarth. 1986. Mechanisms of chlorophyll fluorescence revisited: Prompt or delayed emission from photosystem II with closed reaction centers? *Photosynth. Res.* 10:309–318.
72. Berens, S. J., J. Scheele, W. J. Butler, and D. Magde. 1985. Kinetic modeling of time resolved fluorescence in spinach chloroplasts. *Photochem. Photobiol.* 42:59–68.
73. Butler, W. L., D. Magde, and S. J. Berens. 1983. Fluorescence lifetimes in the bipartite model of the photosynthetic apparatus with alpha, beta heterogeneity in photosystem II. *Proc. Natl. Acad. Sci. USA.* 80:7510–7514.
74. Butler, W. L. 1979. Tripartite and bipartite models of the photochemical apparatus of photosynthesis. *In* Chlorophyll Organization and Energy Transfer in Photosynthesis. Vol. 61. Elsevier/Excerpta Medica, Amsterdam, New York. 237–256.
75. Ried, A., and B. Reinhardt. 1980. Distribution of excitation energy between photosystem I and photosystem II in red algae. 3. Quantum requirements of the induction of a state 2-state 1 transition. *Biochim. Biophys. Acta.* 592:76–86.
76. Kyle, D. J., P. Hayworth, and C. J. Arntzen. 1982. Thylakoid membrane protein phosphorylation leads to a decrease in connectivity between photosystem II reaction centers. *Biochim. Biophys. Acta.* 680:336–342.
77. Haworth, P. 1983. Protein phosphorylation-induced state I-state II transitions are dependent on thylakoid membrane microviscosity. *Arch. Biochem. Biophys.* 226:145–154.
78. Lavorel, J., and P. Joliot. 1972. A connected model of the photosynthetic unit. *Biophys. J.* 12:815–831.
79. Holzwarth, A. R. 1987. A model for the functional antenna organization and energy distribution in the photosynthetic appartus of higher plants and green algae. *Progr. Photosynth. Res. 1:53–60.*